

## A Monte Carlo simulation technique for assessment of earthquake-induced displacement of slopes

H. Fattahi<sup>1\*</sup>, N. Babanouri<sup>2</sup> and Z. Varmazyari<sup>1</sup>

1. Department of Mining Engineering, Arak University of Technology, Arak, Iran

2. Department of Mining Engineering, Hamedan University of Technology, Hamedan, Iran

Received 5 April 2018; received in revised form 18 June 2018; accepted 4 July 2018

\*Corresponding author: h.fattahi@arakut.ac.ir (H. Fattahi).

### Abstract

The dynamic response of slopes against earthquake is commonly characterized by the earthquake-induced displacement of slope (EIDS). The EIDS value is a function of several variables such as the material properties, slope geometry, and earthquake acceleration. This work is aimed at the prediction of EIDS using the Monte Carlo simulation method (MCSM). Hence, the parameters height, unit specific weight, cohesion, friction angle, vibration duration, and maximum horizontal acceleration are used to predict the EIDS values. To do this, a multiple non-linear regression relationship is first derived between EIDS and the independent variables. Then MCSM is performed based on the developed regression equation. The results obtained demonstrate that the stochastic approach used is able to successfully reproduce the EIDS values and calculate the confidence intervals. The average of the measured and simulated values for EIDS was 4.34 cm and 4.48 cm, respectively. Eventually, the results of a performed correlation sensitivity analysis revealed that the maximum horizontal acceleration had the greatest impact on EIDS.

**Keywords:** *Earthquake-Induced Displacements, Slopes, Monte Carlo Simulation, Multiple Non-Linear Regression, Sensitivity Analysis.*

### 1. Introduction

The analysis of earth structures (e.g. slopes) against possible earthquakes is of great importance since the instability of such infrastructures usually has catastrophic human, financial, and environmental consequences [1]. Vulnerable slopes may partially fail in the event of an earthquake of magnitude greater than 4, and they may undergo an overall instability against an earthquake of magnitude greater than 6 [2, 3]. The slope geometry, material properties, and ground vibrations control the degree of earthquake-induced instability of a slope [1]. A large number of research works have addressed the earthquake-induced displacement of slope (EIDS). Saygili and Rathje [4] have presented an empirical model to estimate the slope movements against earthquakes. Lin and Whitman [5] have developed a stepwise procedure to calculate the permanent displacements of sliding blocks caused

by ground accelerations. Rathje and Saygili [6] have carried out a probabilistic analysis of EIDS. Refice and Capolongo [7] have performed a reliability analysis of slope stability against earthquake loads. Al-Homoud and Tahtamoni [8] have considered the uncertainties associated with a 3D slope stability analysis and studied the earthquake-induced movements. Yuan et al. [9] have considered the effect of the acceleration component normal to the sliding surface on earthquake-induced landslide triggering. Babanouri and Dehghani [10] have studied the failure probability and shear strains for a large potentially slide-prone slope in the event of a design earthquake. Bray and Travararou [11] have developed a simplified approach that used a non-linear fully-coupled sliding-block model to produce a semi-empirical relationship for predicting displacements. Bray and Travararou

[12] have presented a straightforward approach to calculate the pseudo-static coefficient as a function of allowable displacement, earthquake magnitude, and spectral acceleration. The common basis of these rationalized approaches is calibration based on allowable displacement. Jibson [13] has divided the methods developed to assess the stability or performance of slopes during earthquakes into three general categories: (1) pseudo-static analysis, (2) stress-deformation analysis, and (3) permanent-displacement analysis. Bojadjeva et al. [14] have studied the landslide hazard and risk assessment considering different water saturation and earthquake scenarios for a selected area in a sub-urban hilly part of Skopje, the capital of Macedonia.

On the other hand, the Monte Carlo simulation method (MCSM) has been widely used to determine uncertainties of geoscience problems. Using MCSM, Jiang et al. [15] have estimated the failure probability of a soil slope with spatially variable properties. Wang et al. [16] have carried out a reliability analysis of slope stability with the help of MCSM and evaluated the impact of the parameters involved. Abbaszadeh et al. [17] have evaluated a reliability index analysis for the Sungun copper mine slope stability based on three uncertainty methods consisting of the Taylor series method, Rosenblueth point estimate method, and MCSM. Sari et al. [18] have successfully used MCSM to anticipate the back break area for a production blasting design. Ghasemi et al. [19], Armaghani et al. [20], and Little and Blair [21] have applied MCSM to predict the blast-induced fly-rock risk in surface mines. Fattahi et al. [22] have assessed the damaged zone of the surrounding underground excavations by coupling MCSM and the ANFIS-subtractive clustering method. Based on the Kuz-Ram equation, Morin and Ficarazzo [23] have carried out a Monte Carlo simulation of the blast fragmentation size. Li and Chu [24] have developed a systematic and probabilistic approach to locate the multiple failure surfaces combining

the traditional limit equilibrium method with MCSM. Mahdiyari et al. [25] have conducted a risk analysis of a slope instability in the presence of seismic loads using MCSM.

This paper presents a research work in which MCSM is used to predict EIDS. First, a regression equation was established to empirically predict EIDS. Then a Monte Carlo simulation was performed based on the developed equation. Finally, in order to evaluate the effect of each parameter involved on EIDS, a sensitivity analysis was carried out.

## 2. Database description

In order to model EIDS in this work, a database of the input and output variables was borrowed from the literature [26]. The original data covering 45 case studies are presented in Table 1. Furthermore, the statistical characterization of the database is provided in Table 2. The database was extracted by analyzing five embankments of slope angle  $\beta = 2:3$  and pore water pressure ratio  $r_u = 0.1$ . The earthquake-induced displacements ( $u$ ) for radius ( $r$ ) = 5, 10, and 15 km, and magnitude ( $M$ ) = 6, 6.5, and 7 Richter were calculated for the five embankments using Eqs. (1) to (3). In this way, a database containing 45 cases was established. Eqs. (1) to (3) take the input parameters of height ( $H$ ), unit specific weight ( $\gamma$ ), cohesion ( $C$ ), angle of internal friction ( $\varphi$ ), significant duration of shaking ( $D_{5-95}$ ), maximum horizontal acceleration ( $k_{max}$ ), and return displacement ( $u$ ). Section 4.2.2 in [26] thoroughly explains the database.

$$\log_{10} \left( \frac{u}{k_{max} D_{5-95}} \right) = 1.87 - 3.477 \frac{k_y}{k_{max}} \quad (1)$$

where  $D_{5-95}$  is the significant duration of shaking, i.e. 5–95% normalized Arias intensity (s),

$$k_{max} = \frac{MHEA}{g} \quad (MHEA: \text{ maximum horizontal equivalent acceleration, representing the amplitude of the mass vibration}), \text{ and } k_y \text{ is the acceleration in which the slope yields [26].}$$

$$\ln(D_{5-95})_{med} = \ln \left[ \frac{\left( \frac{\exp[5.204 + 0.851(M - 6)]}{10^{1.5M + 16.05}} \right)^{\frac{1}{3}}}{15.7 \times 10^6} + 0.0063(r - 10) \right] + 0.8664, \quad \text{For } r > 10 \text{ km} \quad (2)$$

$$\ln(D_{5-95})_{med} = \ln \left[ \frac{\left( \frac{\exp[5.204 + 0.851(M - 6)]}{10^{1.5M + 16.05}} \right)^{\frac{1}{3}}}{15.7 \times 10^6} \right] + 0.8664, \quad \text{For } r < 10 \text{ km} \quad (3)$$

where  $M$  is the earthquake magnitude in Richter and  $r$  is the distance in km.

**Table 1. Original data used for modeling [26].**

Case No.	Input parameters						Output parameter
	H (m)	$\gamma$ (KN/m <sup>3</sup> )	C (KPa)	$\Phi$ (°)	D <sub>5-95</sub>	k <sub>max</sub>	u (cm)
1	12	22	8	35	7.9	0.24	0.25
2	12	22	8	35	8.35	0.2	0.06
3	12	22	8	35	9.55	0.13	0.0008
4	12	22	8	35	11.1	0.33	2.7
5	12	22	8	35	11.5	0.27	0.82
6	12	22	8	35	12.7	0.18	0.036
7	12	22	8	35	16	0.45	18.16
8	12	22	8	35	16.4	0.37	7.37
9	12	22	8	35	17.65	0.24	0.55
10	10	22	5	35	7.9	0.24	1.19
11	10	22	5	35	8.35	0.2	0.4
12	10	22	5	35	9.55	0.13	0.014
13	10	22	5	35	11.1	0.33	8.45
14	10	22	5	35	11.5	0.27	3.31
15	10	22	5	35	12.7	0.18	0.3
16	10	22	5	35	16	0.45	42
17	10	22	5	35	16.4	0.37	20.4
18	10	22	5	35	17.65	0.24	2.7
19	10	21	5	36	7.9	0.24	0.55
20	10	21	5	36	8.35	0.2	0.16
21	10	21	5	36	9.55	0.13	0.003
22	10	21	5	36	11.1	0.33	4.84
23	10	21	5	36	11.5	0.27	1.68
24	10	21	5	36	12.7	0.18	0.1
25	10	21	5	36	16	0.45	27.84
26	10	21	5	36	16.4	0.37	12.4
27	10	21	5	36	17.65	0.24	1.24
28	8	22	6	36	7.9	0.24	0.094
29	8	22	6	36	8.35	0.2	0.02
30	8	22	6	36	9.55	0.13	0.0001
31	8	22	6	36	11.1	0.33	1.34
32	8	22	6	36	11.5	0.27	0.35
33	8	22	6	36	12.7	0.18	0.001
34	8	22	6	36	16	0.45	10.8
35	8	22	6	36	16.4	0.37	3.94
36	8	22	6	36	17.65	0.24	0.2
37	6	21	5	35	7.9	0.24	0.07
38	6	21	5	35	8.35	0.2	0.013
39	6	21	5	35	9.55	0.13	7.34
40	6	21	5	35	11.1	0.33	1.07
41	6	21	5	35	11.5	0.27	0.26
42	6	21	5	35	12.7	0.18	0.006
43	6	21	5	35	16	0.45	9.24
44	6	21	5	35	16.4	0.37	3.24
45	6	21	5	35	17.65	0.24	0.16

**Table 2. Statistics of input and output datasets.**

	Parameter	Unit	Symbol	Min.	Max.
<b>Inputs</b>	Height	m	H	6	12
	Special Weight	KN/m <sup>3</sup>	$\gamma$	21	22
	Cohesion	KPa	C	5	8
	Angle of friction	°	$\phi$	35	36
	Period of time	-	D <sub>5-95</sub>	7.9	17.65
	Horizontal acceleration	m/s <sup>2</sup>	K <sub>max</sub>	0.13	48
<b>Output</b>	Displacement	cm	U	0.001	42

### 3. Developing an EIDS predictive model

In order to the simulate EIDS using MCSM, an empirical equation is first required to be developed [18, 20, 25]. Therefore, the non-linear multiple regression (MNLR) analysis was used. The parameters  $H$ ,  $\gamma$ ,  $C$ ,  $\phi$ ,  $D_{5-95}$ , and  $k_{max}$  were considered as the input variables, and EIDS was the dependent parameter. 80% of the datasets were considered as the training data used for building the model, and 20% of them were allocated to the testing data used for assessing the model performance for unseen cases. The following formula was fitted over the data using SPSS v16 [27].

$$U(cm) = 0.04 + \exp(9.8 + 0.41H + 0.2\gamma - 0.67C + 0.52\phi + 0.1D_{5-95} + 12.48K_{max}) \quad (4)$$

The performance of Eq. (4) was examined using the squared correlation coefficient ( $R^2$ ), mean square error (MSE), root mean square error (RMSE), and variance account for (VAF), defined as follow, respectively:

$$R^2 = 1 - \frac{\sum_{i=1}^N (y - y')^2}{\sum_{i=1}^N (y - \tilde{y})^2} \quad (5)$$

$$MSE = \frac{1}{N} \sum_{i=1}^N (y - y')^2 \quad (6)$$

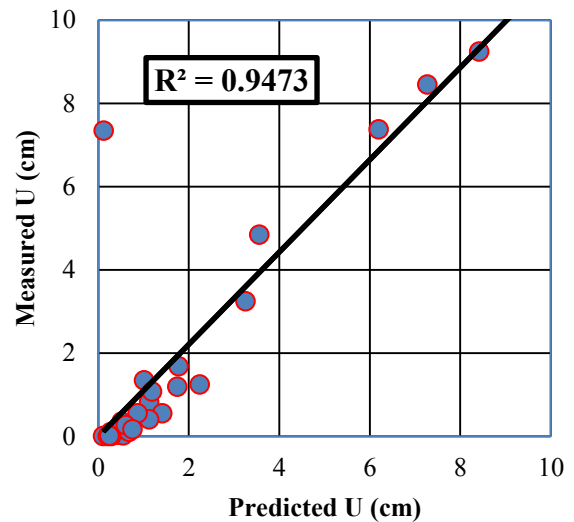
$$RMSE = \sqrt{\frac{1}{N} \sum_{i=1}^N (y - y')^2} \quad (7)$$

$$VAF = \left( 1 - \frac{\text{var}(y - y')}{\text{var}(y)} \right) \quad (8)$$

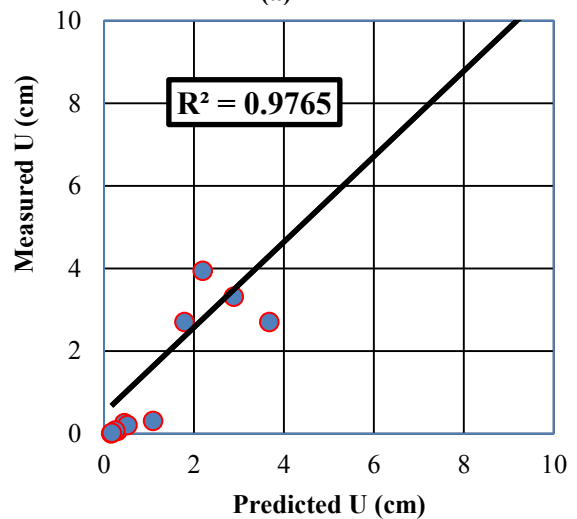
where  $y$  is the measured value for the dependent parameter,  $y'$  and  $\tilde{y}$  stand for the predicted values and their mean, respectively, and  $N$  specifies the number of data. The above-mentioned indices were computed for Eq. (4) in the training and testing phases. The performance indices obtained in Table 3 demonstrate the strong performance of the model in the indirect estimation of EIDS. Furthermore, correlations between the measured and predicted values of EIDS for the testing and training phases are shown in Figure 1.

**Table 3. Performance of regression model for predicting EIDS.**

Type data	$R^2$	MSE	RMSE	VAF
Training data	0.95	2.476	1.573	0.94
Testing data	0.98	3.646	1.909	0.97



(a)



(b)

**Figure 1. Correlation between measured and predicted EIDS values for a) training data b) testing data.**

### 4. Monte Carlo simulation of EIDS

Contrary to a deterministic modeling in which a fixed value is considered for each influencing parameter, a distribution of values is considered for any input parameter in the Monte Carlo simulation according to its pre-defined statistical characterization. Then a large number (commonly 1000) of realizations of the system and their corresponding response are obtained. In this way, MCSM provides identification of the uncertainties associated with an estimator model [19, 20, 28, 29].

In this work, the @Risk software was used to perform the Monte Carlo simulation of EIDS. The developed regression relationship was used as the estimation model. Each one of the model inputs

( $H, \gamma, C, \varphi, D_{5-95}$ , and  $k_{max}$ ) was specified with a continuous probability distribution. In order to find the best-representing distribution, the Expon, Pareto, Triang, and InvGauss functions were examined. The best-fitted probability distribution functions of the input variables are given in Table 4.

The software @Risk provides two schemes for sampling, namely Latin Hypercube sampling (LHS) and simple random sampling. In LHS, the stratified sampling is performed, which requires a lower number of sample generation, and yields a more accurate representation of the prescribed probability distributions [30]. Hence, LHS with 6,000 iterations was carried out in this work to ensure a good realization of the distribution functions. As a result, 6,000 different possible combinations of independent parameter values were evaluated in the Monte Carlo simulation.

The existence of correlation between the input parameters may significantly influence the simulation results. Therefore, the cross-correlation of the input parameters was also investigated

(Table 5). For the sample generation to be rational, the existing correlations between the input parameters are required to be accounted for; otherwise, the generated samples would be quite random.

The EIDS distribution model obtained using MCSM together with the summary statistics are shown in Figure 2. It was found that the LogNormal distribution was the best-fitting model. In addition, the EIDS values were found to range from a minimum of 0.04 cm to a maximum of 111.04 cm with an average of 4.48 cm. As it can be seen, the EIDS values obtained by the simulated model vary within a quite wide range. At the 90% confidence level, the EIDS values will not exceed 20.97 cm. Different variation ranges of EIDS can be extracted from the analysis results at different levels of confidence. Moreover, the EIDS values obtained by measurement, the MNL model, and MCSM simulation are compared in Figure 3. This figure proves that the proposed MCSM is capable of reproducing the EIDS values properly.

**Table 4. Probability distribution functions of input parameters.**

Model input	Best-fitted function
H	Expon (k, sigma): k = 3.2, sigma = 5.928
$\gamma$	Pareto( $\alpha, \beta$ ): $\alpha = 35.827, \beta = 21$
C	Triang( $\alpha, \beta, \sigma$ ): $\alpha = 5, \beta = 5, \sigma = 8.649$
$\varphi$	Triang( $\alpha, \beta, \sigma$ ): $\alpha = 35, \beta = 35, \sigma = 36.4$
$D_{5-95}$	InvGauss(A, B, C): A = 7.1617, B = 23.666, C = 5.1883
$k_{max}$	Expon (k, sigma): k = 0.1377, sigma = 0.1269

**Table 5. Spearman's correlation coefficients for model inputs.**

	H	$\gamma$	C	$\varphi$	$D_{5-95}$	$k_{Max}$
H	1					
$\gamma$	0.48	1				
C	0.60	0.56	1			
$\varphi$	-0.08	-0.16	-0.21	1		
$D_{5-95}$	0.0	0.0	0.0	0.0	1	
$k_{Max}$	0.0	0.0	0.0	0.0	0.55	1

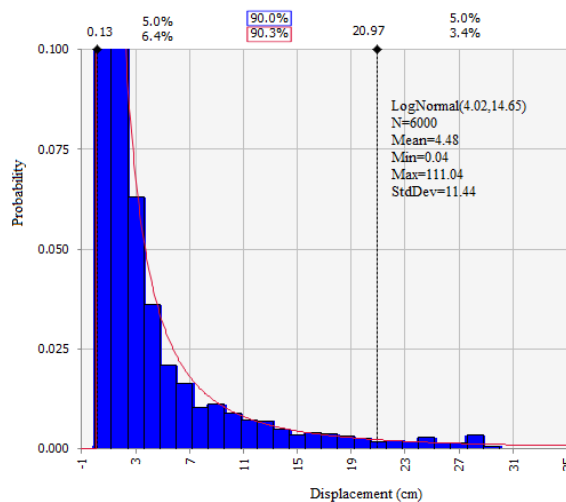


**Figure 2. Histogram of EIDS achieved by MCS along with statistical details.**

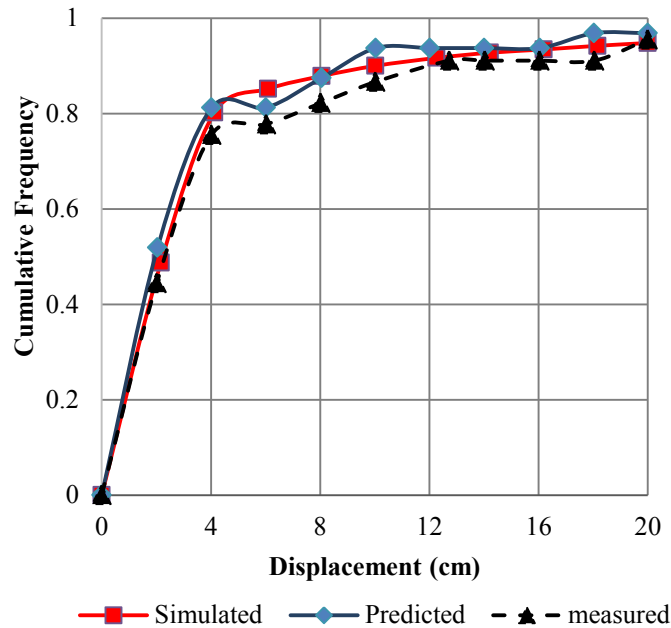


Figure 3. Comparison of the cumulative frequency of measured, predicted, and simulated values of EIDS.

### 5. Correlation sensitivity analysis

A correlation sensitivity analysis was carried out to determine the role of each influencing parameter in the EIDS prediction. The rank-order correlations between each one of the input parameters and the simulated EIDS values were calculated using the STATISTICA software package. In order to do this, the two variables (EIDS and one of the input parameters) are first ranked. Then the correlation between their ranks is computed [25, 20]. In this way, the strength and direction of sensitivity of EIDS to the input parameters are measured (Table 6). The value for the rank-order correlation varies between  $-1$  and  $+1$ . As it can be seen, the most influential parameter is  $k_{max}$  with a correlation coefficient of 0.696, and then EIDS is sensitive to  $D_{5-95}$ ,  $C$ ,  $\gamma$ ,  $H$ , and  $\phi$ , respectively.

Table 6. Results of correlation sensitivity analysis.

Name of variable	Correlation coefficient
$k_{max}$	0.696 (1)
$D_{5-95}$	0.437 (2)
$H$	0.128 (3)
$C$	-0.115 (4)
$\phi$	-0.069 (5)
$\gamma$	0.044 (6)

### 6. Conclusions

The displacements induced by an earthquake are important because the displacements can be very large and result in severe damages to the earth and earth-supported structures. In this work, MCSM

was used to evaluate/predict EIDS. For this aim, a total of 45 datasets were extracted by analyzing five embankments of slope angle  $\beta = 2:3$  and pore water pressure ratio  $r_u = 0.1$ . In this work, the parameters having the most influence on EIDS (i.e.  $k_{max}$ ,  $D_{5-95}$ ,  $C$ ,  $\gamma$ ,  $H$ , and  $\phi$ ) were used as the independent parameters. In the first step, an empirical equation was developed between EIDS and the independent variables using the MNLR technique. The results of the values predicted using the constructed equation were in good agreement with the actual data, demonstrating the reliability of the developed MNLR model. Then this equation was used in MCSM. The results obtained for the predicted and simulated EIDS values were very similar to the measured ones in all the data cases. The average of the simulated EIDS values was obtained to be 4.48 cm, while the actual EIDS values had an average of 4.34 cm. Furthermore, the results obtained revealed that there was a positive correlation between EIDS and  $k_{max}$ ,  $D_{5-95}$ ,  $\gamma$ , and  $H$ . On the other hand,  $C$  and  $\phi$  had negative correlations with EIDS. Furthermore, the sensitivity analysis demonstrated that  $k_{max}$ , among the other parameters, had the most influence on the EIDS value. It is noticeable that due to the nature of the problem, the model/equation proposed in this work cannot be applied directly to other conditions, and should only be used for the mentioned parameters and their ranges. In order to do simulation in other slopes, the process presented in this work should be reconsidered.

## References

- [1]. Ambraseys, N. and Srbulov, M. (1995). Earthquake induced displacements of slopes. *Soil Dynamics and Earthquake Engineering*. 14 (1): 59-71.
- [2]. Keefer, D.K. (1984). Landslides caused by earthquakes. *Geological Society of America Bulletin*. 95 (4): 406-421.
- [3]. Jibson, R.W. (1993). Predicting earthquake-induced landslide displacements using Newmark's sliding block analysis. *Transportation research record*. pp. 9-17.
- [4]. Saygili, G. and Rathje, E.M. (2008). Empirical predictive models for earthquake-induced sliding displacements of slopes. *Journal of geotechnical and geoenvironmental engineering*. 134 (6): 790-803.
- [5]. Lin, J.S. and Whitman, R.V. (1986). Earthquake induced displacements of sliding blocks. *Journal of Geotechnical engineering*. 112 (1): 44-59.
- [6]. Rathje, E.M. and Saygili, G. (2009). Probabilistic assessment of earthquake-induced sliding displacements of natural slopes. *Bulletin of the New Zealand Society for Earthquake Engineering*. 42 (1): 18.
- [7]. Refice, A. and Capolongo, D. (2002). Probabilistic modeling of uncertainties in earthquake-induced landslide hazard assessment. *Computers & Geosciences*. 28 (6): 735-749.
- [8]. Al-Homoud, A. and Tahtamoni, W. (2000). Reliability analysis of three-dimensional dynamic slope stability and earthquake-induced permanent displacement. *Soil Dynamics and Earthquake Engineering*. 19 (2): 91-114.
- [9]. Yuan, R.M., Tang, C.L. and Deng, Q.H. (2015). Effect of the acceleration component normal to the sliding surface on earthquake-induced landslide triggering. *Landslides*. 12 (2): 335-344.
- [10]. Babanouri, N. and Dehghani, H. (2017). Investigating a potential reservoir landslide and suggesting its treatment using limit-equilibrium and numerical methods. *Journal of Mountain Science*. 14 (3): 432-441.
- [11]. Bray, J.D. and Travasarou, T. (2007). Simplified procedure for estimating earthquake-induced deviatoric slope displacements. *Journal of geotechnical and geoenvironmental engineering*. 133 (4): 381-392.
- [12]. Bray, J.D. and Travasarou, T. (2009). Pseudostatic coefficient for use in simplified seismic slope stability evaluation. *Journal of geotechnical and geoenvironmental engineering*. 135 (9): 1336-1340.
- [13]. Jibson, R.W. (2011). Methods for assessing the stability of slopes during earthquakes- A retrospective. *Engineering Geology*. 122 (1-2): 43-50.
- [14]. Bojadjieva, J., Sheshov, V. and Bonnard, C. (2018). Hazard and risk assessment of earthquake-induced landslides- case study. *Landslides*. 15 (1): 161-171.
- [15]. Jiang, S.H., Li, D.Q., Cao, Z.J., Zhou, C.B. and Phoon, K.K. (2014). Efficient system reliability analysis of slope stability in spatially variable soils using Monte Carlo simulation. *Journal of geotechnical and geoenvironmental engineering*. 141 (2): 04014096.
- [16]. Wang, Y., Cao, Z. and Au, S.K. (2010). Practical reliability analysis of slope stability by advanced Monte Carlo simulations in a spreadsheet. *Canadian Geotechnical Journal*. 48 (1): 162-172.
- [17]. Abbaszadeh, M., Shahriar, K., Sharifzadeh, M. and Heydari, M. (2011). Uncertainty and Reliability Analysis Applied to Slope Stability: A Case Study From Sungun Copper Mine. *Geotechnical and Geological Engineering*. 29 (4): 581-596.
- [18]. Sari, M., Ghasemi, E. and Ataei, M. (2014). Stochastic modeling approach for the evaluation of backbreak due to blasting operations in open pit mines. *Rock Mechanics and Rock Engineering*. 47 (2): 771-783.
- [19]. Ghasemi, E., Sari, M. and Ataei, M. (2012). Development of an empirical model for predicting the effects of controllable blasting parameters on flyrock distance in surface mines. *International Journal of Rock Mechanics and Mining Sciences*. 52: 163-170.
- [20]. Armaghani, D.J., Mahdiyar, A., Hasanipanah, M., Faradonbeh, R.S., Khandelwal, M. and Amnieh, H.B. (2016). Risk assessment and prediction of flyrock distance by combined multiple regression analysis and monte carlo simulation of quarry blasting. *Rock Mechanics and Rock Engineering*. 49 (9): 3631-3641.
- [21]. Little, T. and Blair, D. (2010). Mechanistic Monte Carlo models for analysis of flyrock risk. *Rock fragmentation by blasting*. 9: 641-647.
- [22]. Fattahi, H., Shojaee, S., Farsangi, M.A.E. and Mansouri, H. (2013). Hybrid Monte Carlo simulation and ANFIS-subtractive clustering method for reliability analysis of the excavation damaged zone in underground spaces. *Computers and Geotechnics*. 54: 210-221.
- [23]. Morin, M.A. and Ficarazzo, F. (2006). Monte Carlo simulation as a tool to predict blasting fragmentation based on the Kuz-Ram model. *Computers & Geosciences*. 32 (3): 352-359.
- [24]. Li, L. and Chu, X. (2016). Locating the Multiple Failure Surfaces for Slope Stability Using Monte Carlo Technique. *Geotechnical and Geological Engineering*. 34 (5): 1475-1486.
- [25]. Mahdiyar, A., Hasanipanah, M., Armaghani, D.J., Gordan, B., Abdullah, A., Arab, H. and Majid, M.Z.A. (2017). A Monte Carlo technique in safety assessment of slope under seismic condition. *Engineering with Computers*. pp. 1-11.

[26]. Ferentinou, M. and Sakellariou, M. (2007). Computational intelligence tools for the prediction of slope performance. *Computers and Geotechnics*. 34 (5): 362-384.

[27]. SPSS, S. (2008). version 16.0 for Windows. SPSS Inc, Chicago III.

[28]. Dunn, W.L. and Shultis, J.K. (2009). Monte Carlo methods for design and analysis of radiation detectors. *Radiation Physics and Chemistry*. 78 (10): 852-858.

[29]. Bianchini, F. and Hewage, K. (2012). Probabilistic social cost-benefit analysis for green roofs: a lifecycle approach. *Building and environment*. 58: 152-162.

[30]. Liu, M.M. (2014). Probabilistic prediction of green roof energy performance under parameter uncertainty. *Energy*. 77: 667-674.

## تکنیک شبیه‌سازی مونت کارلو برای ارزیابی جابجایی ناشی از زلزله شیروانی‌ها

هادی فتاحی<sup>۱\*</sup>، نیما بابانوری<sup>۲</sup> و زهرا ورمزیاری<sup>۱</sup>

۱- گروه مهندسی معدن، دانشگاه صنعتی اراک، اراک، ایران

۲- گروه مهندسی معدن، دانشگاه صنعتی همدان، اراک، ایران

ارسال ۲۰۱۸/۴/۵، پذیرش ۲۰۱۸/۷/۴

\* نویسنده مسئول مکاتبات: h.fattahi@arakut.ac.ir

---

### چکیده:

پاسخ دینامیکی شیروانی‌ها در برابر زلزله معمولاً توسط جابجایی ناشی از زلزله شیروانی مشخص می‌شود. مقادیر جابجایی ناشی از زلزله شیروانی تابع چندین متغیر مانند ویژگی‌های مصالح، ابعاد هندسی شیروانی و شتاب زلزله است. هدف از این پژوهش پیش‌بینی جابجایی ناشی از زلزله شیروانی با استفاده از روش شبیه‌سازی مونت کارلو است. برای این منظور پارامترهای ارتفاع، وزن مخصوص، چسبندگی، زاویه اصطکاک داخلی، مدت زمان لرزش و ماکزیمم شتاب افقی زلزله برای پیش‌بینی جابجایی ناشی از زلزله شیروانی مورد استفاده قرار گرفته است. برای انجام این کار، ابتدا رابطه رگرسیون غیرخطی چند متغیره بین جابجایی ناشی از زلزله شیروانی و متغیرهای مستقل به دست آمد. سپس بر اساس معادله به دست آمده روش شبیه‌سازی مونت کارلو به کار گرفته شد. نتایج به دست آمده نشان می‌دهد که رویکرد تصادفی استفاده شده با موفقیت می‌تواند جابجایی ناشی از زلزله شیروانی را محاسبه کند. به طوری که میانگین مقادیر اندازه‌گیری و شبیه‌سازی شده جابجایی ناشی از زلزله شیروانی به ترتیب ۴/۳۴ سانتیمتر و ۴/۴۸ سانتیمتر است. در نهایت نیز آنالیز حساسیت انجام شده روی پارامترها نشان می‌دهد که ماکزیمم شتاب افقی بیشترین تأثیر را روی جابجایی ناشی از زلزله شیروانی دارد.

**کلمات کلیدی:** جابجایی ناشی از زلزله، شیروانی، شبیه‌سازی مونت کارلو، رگرسیون غیرخطی چند متغیره، آنالیز حساسیت.

---